Optical Design of a Compact Image Acquisition Device for Mobile Diabetic Retinopathy Screening

David Melo[1,2], João Costa[2], Filipe Soares[2] and Pedro Vieira[1]
[1]*Department of Physics, Faculdade de Ciências e Tecnologia, Universidade Nova de Lisboa, Quinta da Torre, 2829-516, Caparica, Portugal*
[2]*Fraunhofer Portugal AICOS, Rua Alfredo Allen, 455/461, 4200-135, Porto, Portugal*

Keywords: Diabetic Retinopathy, Fundus Camera, Optical System Design, Mechanical Prototyping.

Abstract: Imaging the eye retina is critical to diagnose various pathologies, particularly Diabetic Retinopathy, which is the leading cause of avoidable blindness in the world. Accessing the retina can be achieved through ophthalmoscopes with small field-of-view or Optical Coherence Tomography and fundus cameras, which are larger and expensive. The image acquisition through tabletop fundus cameras is the preferred method for retinopathy screening. However, these devices tend to be cumbersome and require expertise for operation, limiting its broad application. In this paper, a compact optical system was designed for a handheld and smartphone-based fundus camera prototype called EyeFundusScope, with the main goal of low-cost and high coverage screening. The key features for the compact optical system are the mobile and non-mydriatic acquisition of fundus images by a smartphone camera, with high field-of-view. The simplicity of the optical system was accomplished by a three lens system setup, simulated using ray tracing software. The results reveal a system with only a few aberrations in the periphery but with a good resolution at the center of 41° field-of-view. Besides the optical system, a mechanical prototype was designed with the purpose of being 3D printed and easily portable.

1 INTRODUCTION

1.1 Diabetic Retinopathy

The eye retina is the only structure in the body where vessels can be directly seen, without intrusive procedures. Imaging this structure is extremely important in the diagnosis of various pathologies, particularly Diabetic Retinopathy. This is a microvascular disease caused by the diabetes mellitus condition, affecting 76% of the diabetic patients for longer than 20 years (Cheung et al., 2010) and being the leading cause of blindness in adults with working age (Bunce and Wormald, 2006). It is characterized by the loss of perycites and by a progressive capillary occlusion that occurs mostly without symptoms. The capillary occlusion can lead to retinal ischemia and to the breakdown of the blood-retinal-barrier (Tarr et al., 2013).

The disease can be divided in two different stages: Non-proliferative and Proliferative (Kauppi, 2010). The first is characterized by abnormalities in the blood vessels materialized in the leakage of substances from the lumen of the vessels to the retinal epithelium. The leakages may be the blood itself leading to microaneurysms and intraretinal hemorrhages, and lipids leading to hard and soft Exudates (Kauppi, 2010; Cunha-Vaz, 2007; Giancardo, 2012). The Proliferative stage is characterized by the creation of new blood vessels surrounding occluded regions (neovascularization). The new blood vessels, being more fragile than the previous ones, increase the risk of bleeding and do not solve retinal ischemia (Giancardo, 2012). In the Proliferative stage there is also the formation of fibrous tissue that while contracting can provoke retinal detachment (do Prado et al., 2002).

Several types of instruments can perform ophthalmological examination, but for the diagnosis of Diabetic Retinopathy the use of Fundus Camera is preferred (Salz and Witkin, 2015).

The asymptomatic profile of the initial progression of diabetic retinopathy is problematic for diagnostic purposes. On the other hand, the success of early treatment provides a large incentive to implement population-based screening programs for diabetic patients. In these programs, images of the patient retinas are acquired and assessed by qualified technicians and ophthalmologists, which lead to high

Melo, D., Costa, J., Soares, F. and Vieira, P.
Optical Design of a Compact Image Acquisition Device for Mobile Diabetic Retinopathy Screening.
DOI: 10.5220/0006592200630070
In *Proceedings of the 11th International Joint Conference on Biomedical Engineering Systems and Technologies (BIOSTEC 2018) - Volume 1: BIODEVICES*, pages 63-70
ISBN: 978-989-758-277-6

costs due to the required use of expensive and bulky equipment, and the laborious task of manual analysis by scarcely available medical personnel. The prototype EyeFundusScope, currently under investigation by Fraunhofer Portugal AICOS, aims to address these issues by researching on a self-contained solution comprising automated retinopathy detection with a low cost optical attachment to a smartphone for retinal image acquisition. The major goal is to improve patient access to early treatment and decrease the burden of screening actions on healthcare systems.

The present work is a contribution to a compact optical system, proposed to achieve this goal. The resolution of the optical system is intended to be sufficient to distinguish microaneurysms, the small structures that commonly appear in the earliest stages of Diabetic Retinopathy and whose size varies from 25 to 125 micrometers (Li et al., 2006).

1.2 Fundus Camera

A Fundus Camera is a device that allows the observation of the structures and the blood vessels in the ocular fundus, being employed in the diagnosis of several pathologies (like Diabetic Retinopathy, described in section 1.1) (Pérez et al., 2012).

When compared with other eye examination devices, a Fundus Camera enables patient documentation and easy follow, as well as allowing analysis of a great extent of the patient retina, due to the wide field-of-view empowered by the usage of indirect ophthalmoscopy principles, hardly achievable with direct ophthalmoscopy methods (Benbassat et al., 2012), (Phillips, 1984).

The importance of the fundus examination can be seen in many medicine fields and not only in ophthalmology. Since the retina is the human body structure where the vessels can more easily be seen with no use of ionizing radiation (Pérez et al., 2012), fields like Neurology and Cardiology can also use the capabilities of a Fundus Camera (Patton et al., 2005). A handheld portable Fundus Camera can also be a crucial tool in the development of telemedicine (Pérez et al., 2012).

In the present work, we propose a simple Fundus Camera optical system, using only 3 lenses, allowing a 40º field-of-view with minimized aberrations and no need of pupil dilation. Generally, to have good capabilities, indirect ophthalmoscopes use a considerably high number of lenses (Tran et al., 2012). In this work, to diminish the production costs, only the fundamental components of a Fundus Camera were used. A field-of-view of at least 40° is desired, since this is generally considered an adequate tradeoff between sufficient retinal area imaged and enough resolution for analysis of finer retinal features, thus allowing obtaining clinical meaningful conclusions about eventual abnormalities. A diagram with these components is presented in Figure 1. The software used for the Optical Simulation was BEAM IV, an Optical Ray Tracer developed by Stellar Software.

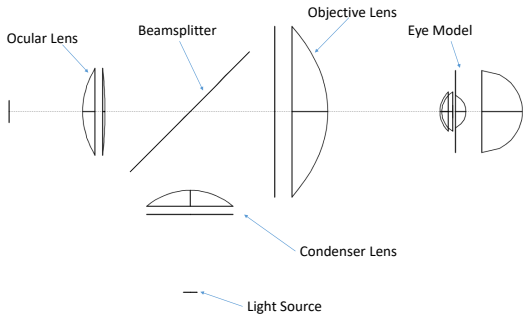

Figure 1: Demonstration of the fundamental components in the Fundus Camera prototype.

1.3 Optical Principles

To reach an optimal optical system several lenses types were tested. To simulate them according to the characteristics supplied by the manufacturers, the thin lens approximation was used. This approximation neglects the thickness of the lens and considers that the unit planes pass through the axial point of the infinitely thin lens (Jenkins and White, 1957). Considering that the media on both sides of the lens is the same, the following equation can be used to describe it (Born and Wolf, 1999).

Lens-Maker's Formula

$$P_{lens} = \frac{n_{lens} - n_0}{n_0}\left(\frac{1}{R_1} - \frac{1}{R_2}\right) \quad (1)$$

Where n_0 is the refractive index of the surrounding medium, the air in this case, equal to 1, n_{lens} is the refractive index of the lens, R_1 is the radius of curvature of the first surface and R_2 is the radius of curvature of the second surface. The P_{lens} is the refractive power in diopters.

To simulate a Fundus Camera optical system, the optical path taken by the rays is separated in two different ones by the usage of a beamsplitter (Tran et al., 2012). The path that describes how the rays illuminate the retina is called *illumination path* and the path describing how the rays go from the retina to the smartphone camera is called *imaging path*. To simulate them two different approaches were tested, the *4-extreme model* for the illumination, and the *parallel rays model* for the imaging path (see Figure 2). The 4-extreme model assumes that the light source emits

from a single point with a certain aperture previously declared by the manufacturer. The angles for which the relative luminous intensity is bellow half the maximum intensity can be neglected.

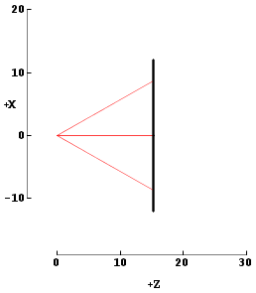

Figure 2: Demonstration of the 4-extremes model along the x-axis.

The parallel rays model assumes that when two rays focused at some point reach a lens they are collimated and leave the lens with the same direction and parallel with each other. In Figure 3 one of the applications of this model is demonstrated, showing rays focused at some point, leaving the pupil parallel.

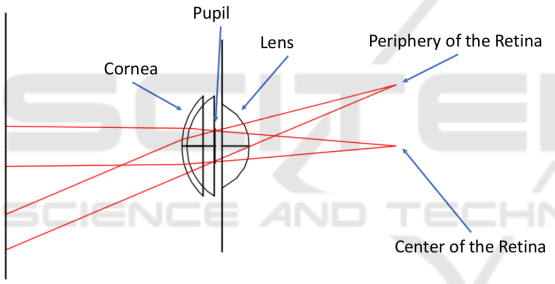

Figure 3: Demonstration of the parallel rays model. In this figure rays are focused on the retina, leaving the pupil collimated and parallel.

1.4 Related Work

Recently, the features of handheld Fundus Camera prototypes have increased significantly when compared with the traditional tabletop fundus cameras (Tran et al., 2012), proving as an helpful instrument in the diagnosis of many pathologies related with the retina and facilitating telemedicine applications (Quellec et al., 2016; Jin et al., 2017). This improvement of the capabilities of handheld devices led to a variety of different approaches. Some examples that reflect the recent scientific development are:

- Nonmydriatic Fundus Camera Based on the Raspberry Pi® Computer: Uses the Raspberry Pi® camera module coupled with a Condenser Lens to perform fundus imaging with a very low production cost (Shen and Mukai, 2017).
- Eye-Selfie: By using internal fixation points as targets, it allows a self-performed acquisition of the fundus photography, completely by the patient (Swedish et al., 2015).

There are already, some fundus camera prototypes available in the market but most, present one of the following issues:

- Low Field Of View, as for the D-EYE ophthalmoscope (D-EYE S.r.l,).
- Require pupil dilation, as for the Volk inView (Volk Optical Inc., a).
- High price, as for the Volk Pictor Plus (Volk Optical Inc., b).

The system we propose differs from the previous approaches by using a smartphone for non-mydriatic, high field-of-view retinal image acquisition. The use of a smartphone instead of custom electronic devices for image capture and processing allows a substantial decrease in costs while allowing for a very high image quality and resolution, thus guaranteeing the cost-effectiveness of the overall solution.

2 TOOLS AND METHODS

2.1 Eye Model

To guarantee a satisfactory field-of-view, an accurate model of the eye is needed. The eye has two refractive lenses, the cornea and the crystalline lens. Based on the literature (Atchison and Smith, 2000) and following a similar approach to (Tocci, 2007), a model of the eye was created in BEAM IV considering the radius of curvature, diameter and asphericity coefficients of all the structures relevant for ray tracing. The pupil has been designed with a 4 mm diameter to simulate a non-mydriatic acquisition with no visible light and is coincident with the lens anterior surface. The chromatic aberrations from the eye were neglected as the change in diopters at different wavelengths were not considered significant in the scope of this work (Atchison and Smith, 2000).

The defined structures of the eye, as represented in Figure 4, are:

- Corneal Anterior surface:
  Diameter = 11.50 mm
  Radius of Curvature = 7.75 mm
  Asphericity coefficient = -0.2
- Corneal Posterior surface:
  Diameter = 11.50 mm
  Radius of Curvature = 6.8 mm
  Asphericity coefficient = 0

- Pupil/ Lens Anterior surface:
  Diameter = 4 mm
  Radius of Curvature = 10 mm
  Asphericity coefficient = -0.94
- Lens Posterior Surface:
  Diameter = 9 mm
  Radius of Curvature = -6 mm
  Asphericity coefficient = 0.96
- Retina:
  Diameter = 24 mm
  Radius of Curvature = 12 mm
  Asphericity coefficient = 0

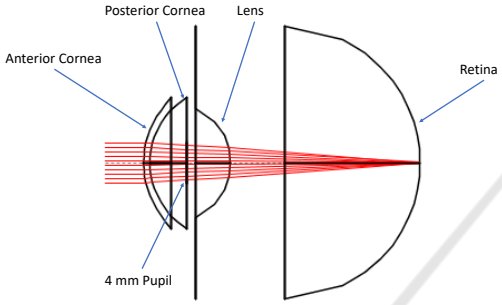

Figure 4: BEAM IV simulation of the eye model used with collimated rays being focused on the retina.

2.2 Illumination Path

For the illumination path the main goal is a 40° field-of-view with a uniform illumination of the retina. The diagram of the illumination path is represented in Figure 5. The image is obtained using a white visible LED but, to allow a non-mydriatic acquisition, a Near Infrared (NIR) LED is used, helping the examiner to perform alignment of the device with the eye and to find the area of the retina to be imaged. As the NIR LED is simply used for guidance, only the Visible LED imaging and illumination capabilities were evaluated. As in most fundus cameras, there is a lens above the light source to collimate the rays and another lens to focus the rays (Tran et al., 2012). This lens that focuses the rays before reaching the eye is called objective lens and it is where the simulations performed began. To obtain a field-of-view of 40° there is a constraint that the relationship $\frac{WD}{2f}$ should be equal to or larger than sin(20) (see Figure 6), where WD stands for Working Diameter and f means the effective focal length of the lens.

The type of objective lens to choose should minimize spherical aberrations. This condition, coupled with the required numerical aperture, makes Aspheric lenses the only suitable option for the focusing of the rays when reaching the retina. After searching

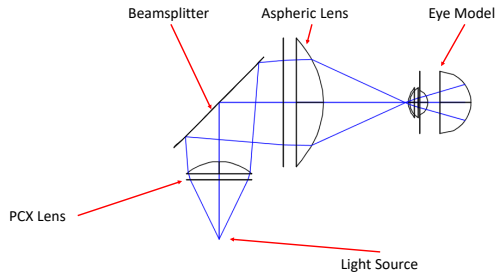

Figure 5: Illumination path and the description of the components used.

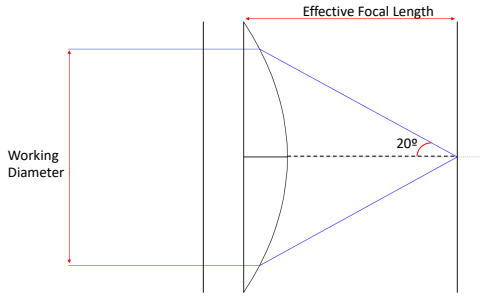

Figure 6: For a 20° half-angle the relationship $\frac{WD}{2f}$ should be equal to or larger than sin(20).

for a lens that fits these requirements we opted to use a Thorlabs aspheric lens with 50.00 mm diameter, 40.00 mm focal length and SLAH-64 glass type, placed 25 mm ahead to the right of the center of the beamsplitter. For the collimation of the rays coming from the light source, the used Condenser lens was an Edmund Optics Plano-Convex Lens with 25.4 mm diameter, 38.1 mm focal length and N-BK7 glass type, placed 47 mm below the center of the beamsplitter.

To check the distance between the objective lens and the human eye, the plane where the rays were in focus was calculated. This plane is called the focal plane and is where the circle of confusion is minimum.

In a theoretically aberration free-system, this is where the pupil should be placed. However, after testing it, was observed that due to spherical aberrations, the intermediate rays reached the optical axis further than the extreme rays, so only 40% reached the retina. This problem was solved by putting the pupil 5 mm after the focal point of the extreme rays. Using this different configuration, 90% of the emitted rays reach the retina and the illumination profile is uniform, as can be observed in Figure 7. The half-angle on the retina calculated was 20.65° leading to a total field-of-view of 41.3°.

In the previous diagrams, the simulated light source emits on a single wavelength (486 nm). As the white light emitted by the LED has a continuous emission spectrum, measurements at the other end of

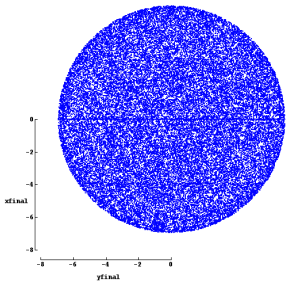

Figure 7: The retinal area illuminated, also called retinal illumination profile, is described, for the configuration represented in Figure 5. The uniformity is noticeable.

the visible spectrum are needed. It was concluded that for red light (656 nm) the system is also optimal with 92% of the rays reaching the retina with an half-angle of 20.57°, leading to a total field-of-view of 41.14 °.

2.3 Imaging Path

For the imaging path the key features desired are the almost complete fulfillment of the Smartphone Camera sensor and the minimization of aberrations.

In order to perform ray tracing analysis of the imaging path, two pairs of parallel rays were considered, one pair parallel with the optical axis and the other with 20° inclination. The distance between the rays, on each pair, was equal to the size of the pupil, 4 mm.

The system was optimized for a LG Nexus 5X camera whose relevant specifications are:

- Horizontal Angle of View : 68.2°
- Vertical Angle of View : 53.1°
- Sensor Size : 1/2.3" (6.17 x 4.55 mm)

The final optical system must guarantee that the Vertical Angle of View is mostly filled with the retinal image, in order to allow the highest possible retinal resolution, essential for the clinical analysis of fine features. The first solution tested was with the Aspheric Lens, described in section 2.2, as an Objective Lens and with a Plano-Convex Lens with 40.0 mm of focal length and 25.4 mm diameter serving as an Ocular. The maximum diameter for the Plano-Convex lens to fit the scope of a compact system was defined to be of 25.4 mm. The system presented too much aberrations and the rays did not reach the Smartphone Camera parallel. To correct the aberrations, as the Objective Lens already fulfilled the requirements for the illumination path, the Ocular Lens was changed. A Best-Form Lens with 40.0 mm focal length, 25.0 Diopters and 25.4 diameter was tested. The aberrations were almost eliminated and the rays reached the smartphone camera parallel to each other, with an inclination of approximately 22°, leading to an angular field-of-view of 44°. The diagram can be seen in Figure 8. The angle in this configuration is inferior to the achieved with the Plano-Convex lens as an ocular, but still wide enough to avoid a significant crop.

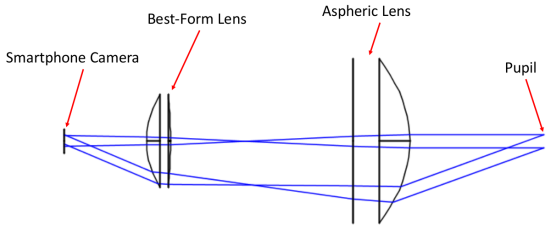

Figure 8: The imaging path with a Best-Form Lens as the Ocular Lens and an Aspheric Lens as the Objective, using the parallel rays model.

In this setup the distance between the Smartphone CMOS sensor and the Best-Form Lens is 22 mm. The distance between the surface of the Best-Form Lens with less curvature and the planar surface of the Aspheric Lens is 50 mm and between the Aspheric lens and the eye is 33 mm.

2.4 Imaging Path for Eyes with Refractive Errors

Eyes with refractive errors present different optical characteristics and so the distance between lenses in the optical system must be adjustable to compensate this.

As the smartphone camera is able to change its focus target distance, the refractive errors were only simulated in the range -5D to +5D. Since one of the possible cause of refractive errors is the size of the eyeball, for the modulation of Myopia the retina was moved 3 mm away from the refractive center of the eye. Concerning the modulation of Hyperopia the eyeball was shortened 3 mm.

In Figure 9, the system configuration for an eye without any refractive error is shown. In Figure 10 and Figure 11, diagrams showing the adjustments done to compensate these refractive errors are shown.

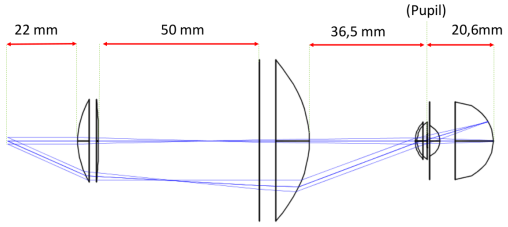

Figure 9: The distances between each components to image an eye without refractive errors.

For the Myopic eye the error is corrected by moving the Objective Lens 5 mm away from the eye.

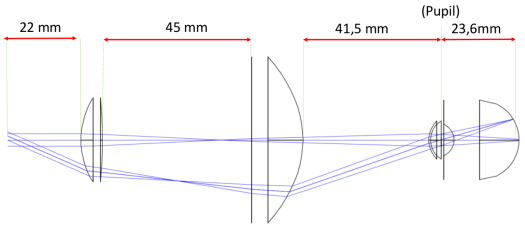

Figure 10: The distances between each components to image an eye with refractive errors (Myopia).

Concerning the Hyperopic eye, the Objective lens is approximated 5 mm to the eye.

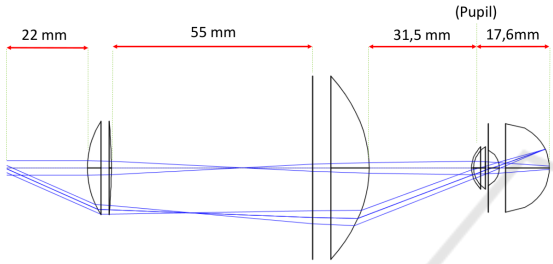

Figure 11: The distances between each components to image an eye with refractive errors (Hyperopia).

2.5 Mechanical Prototyping

The optical system previously described is to be implemented in a 3D printed prototype. The design of the mechanical prototype was developed using Solid Works. The important goals for this prototype are to allow the arrangement of the desired lens, a support for the smartphone that ensures that the camera is centered with the optical path, and the adjustment of the objective lens.

As can be seen in Figure 12, the movements of the Objective are made with a Rack and Pinion system to allow the examiner to precisely search for the working distance, thus allowing the best possible focusing of the retina.

Other solution to allow the movement of the lens would be by the use of threaded surfaces in both sides, so the rotation of the objective ensures a change in the working distance. This approach was rejected because it is expected the future implementation of a piece leaning against the patient forehead, to guarantee the centering with the Optical Path. The rotation of this piece, in contact with the patient, would not be comfortable or, possibly, safe.

Figure 12: Mechanical prototype showing both the smartphone support and the rack and pinion mate.

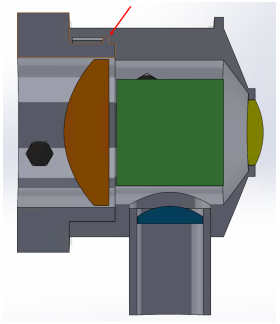

Figure 13: Section view of the prototype. In blue is the PCX Condenser Lens, in yellow the Best-Form Lens, in orange the Aspheric Lens and in green the Beamsplitter. The Beamsplitter is in the form of a cube only for simulation, to simplify the fixation in the mechanical case. The small piece highlighted by the red arrow limits the adjustment between the aspheric lens and the beamsplitter. The configuration presented is for an eye with myopia.

3 RESULTS AND DISCUSSION

3.1 Complete System Designed

The Complete System presented in Figure 14 has the following elements:

- Light Source (Visible or Near Infra-red LED).
- N-BK7 Plano-Convex Lens, 38.1 mm Focal Length, 25.4 mm ϕ, VIS-NIR Coated, 44,00€, Edmund Optics.
- S-LAH64 CNC-Polished Aspheric Lens, 40.0 mm Focal Length, 50 mm ϕ, 392,00€, ThorLabs.
- Beamsplitter 50R/50T 35x35 mm, (≈ 35,00 €).
- N-BK7 Best-Form Lens, 40 mm Focal Length, 25.4 mm ϕ, 39,00€, Thorlabs.

The utilization of aperture stops is dependent on the LEDs beam angle. The aperture can be used to stop the rays emitted by the LED at a wider angle than the necessary for a field-of-view of 40°, preventing reflections and the imaging of undesired areas.

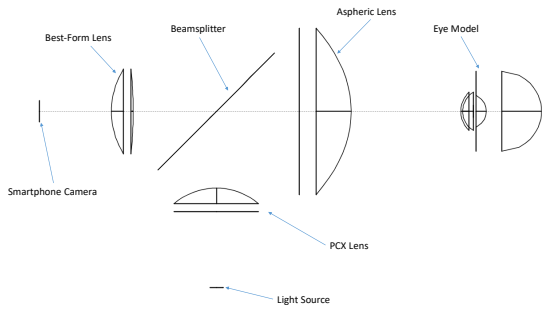

Figure 14: Complete Optical System.

The main features of the developed system are:

- Around 40° field-of-view.
- Non-Mydriatic Acquisition, for a 4 mm pupil size, achievable by using the NIR LED for guidance.
- No significant aberrations (Spherical and Chromatic).
- Uniform Illumination of the Retina.
- Simple and affordable lens system.

3.2 Imaging Path Practical Tests

Some practical tests were performed on the Imaging Path using an Optic Table. A 3.5 mm Iris was used to simulate the pupil and a 38.1 mm focal length Plano-Convex lens was used replacing the eye refractive center. For these tests, only the lights in the room were used to illuminate the target, and this target was a millimeter paper placed at 38 mm from the 38.1 mm Plano-Convex Lens. A black paperboard was used, to prevent the loss of light to the environment and undesired reflections. The smartphone used was a Microsoft Lumia 650 with 63.4° horizontal field-of-view, 49.7° vertical field-of-view and a 3.6 x 2.7 mm sensor size with an 8 Megapixels camera. It was placed at 20 mm from the Best-Form Lens. The results, as shown in Figure 15, demonstrate a system with only a few aberrations in the periphery but with a good resolution at the center showing a field-of-view of about 43°.

The spatial resolution was also assessed. Considering an 8MP resolution camera, the captured picture has 3272×2454 pixels. As the horizontal resolution is superior, the calculations are presented for the vertical resolution. Due to the crop in the vertical field-of-view, the vertical half-angle of view will be of about 17.5°, which would correspond to 6.0 mm in the retina. Thus, the spatial resolution is 4.9 μm, meaning that each pixel contains 4.9 μm of the retinal area, which is sufficient to observe the expected smallest microaneurysms (25 μm). Still based in the previous calculus, the usage of a smartphone camera, instead of a higher resolution camera, is justified by the eye diffraction limit. A much higher resolution would be more expensive and the spatial resolution would start to be close to the eye diffraction limit: for a 5 mm pupil eye receiving light of about 500 nm, this diffraction limit is 1.5 μm (Roorda and Duncan, 2015), close to the resolution calculated.

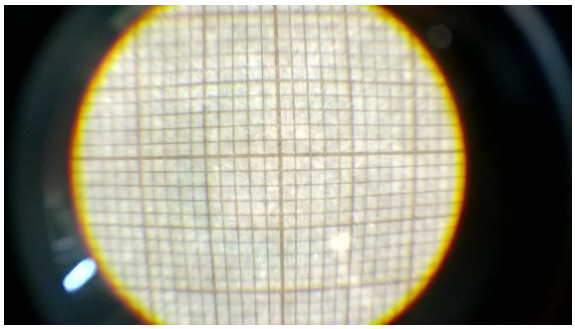

Figure 15: Image obtained by the Microsoft Lumia 650 smartphone demonstrating that at least the centered 15 mm of the target could be imaged.

The quality of the image would be improved if the used millimeter paper could be bent to describe more accurately the retina and diminish spherical aberrations.

3.3 Comparison with other Fundus Cameras

The compact optical system described has a total components cost of about €800, considering the external adapters for the good functioning of the optical system. Fundus Cameras with similar field-of-view and non-mydriatic acquisition, like the Volk Pictor Plus, cost about €10000.

The features of the prototype, coupled with its simplicity and relatively low price compare favorably with the products currently available, can facilitate the provision of healthcare world-wide, and make it an interesting solution for under-developed countries.

4 CONCLUSIONS

It can be concluded that the optical system designed showed satisfactory capabilities in experimental tests, being able to detect the smallest lesions associated with Diabetic Retinopathy. Moreover, it is expected that in the future this device can be a reliable tool in early-stage diagnosis and, indirectly, contributing to an improvement in the treatment of Diabetic Retinopathy cases all over the world.

The 3D-printing of the mechanical prototype described in section 2.5 is expected to be further developed in future work, so that the implementation of the optical system can be performed. After the prototype construction, several "in vivo" tests are expected.

A light hazard measurement, regarding the ISO 15004-2 (ISO 15004-2:2007, 2007) and ISO 10940 (ISO 10940:2009, 2009) norms, for this kind of instruments is also mandatory, being the first for light hazard protection of Ophthalmologic Instruments and the second specifically for Fundus Cameras.

ACKNOWLEDGEMENTS

We would like to acknowledge the financial support obtained from North Portugal Regional Operational Programme (NORTE 2020), Portugal 2020 and the European Regional Development Fund (ERDF) from European Union through the project Symbiotic technology for societal efficiency gains: Deus ex Machina (DEM), NORTE-01-0145-FEDER-000026.

REFERENCES

Atchison, D. and Smith, G. (2000). Optics of the Human Eye. *Butterworth-Heinemann*, page 259.

Benbassat, J., Polak, B. C. P., and Javitt, J. C. (2012). Objectives of teaching direct ophthalmoscopy to medical students. *Acta Ophthalmologica*, 90(6):503–507.

Born, M. and Wolf, E. (1999). *Principles of Optics (7th Ed)*. Cambridge University Press.

Bunce, C. and Wormald, R. (2006). Leading causes of certification for blindness and partial sight in England & Wales. *BMC public health*, 6:58.

Cheung, N., Mitchell, P., and Wong, T. Y. (2010). Diabetic retinopathy. *The Lancet*, 376(9735):124–136.

Cunha-Vaz, J. (2007). Characterization and relevance of different diabetic retinopathy phenotypes. *Developments in Ophthalmology*, 39:13–30.

D-EYE S.r.l. D-EYE Ophthalmoscope.

do Prado, R. S., Figueiredo, E. L., and Magalhaes, T. V. B. (2002). Retinal detachment in preeclampsia. *Arquivos brasileiros de cardiologia*, 79(2):183–186.

Giancardo, L. (2012). Automated fundus images analysis techniques to screen retinal diseases in diabetic patients Docteur de l ' université Automated Fundus Images Analysis Techniques to Screen Retinal Diseases in Diabetic Patients.

ISO 10940:2009 (2009). Ophthalmic instruments - Fundus cameras. Standard, International Organization for Standardization, Geneva, CH.

ISO 15004-2:2007 (2007). Ophthalmic instruments - Fundamental requirements and test methods.Part 2: Light Hazard Protection. Standard, International Organization for Standardization, Geneva, CH.

Jenkins, F. and White, H. (1957). *Fundamentals of optics*. McGraw-Hill.

Jin, K., Lu, H., Su, Z., Cheng, C., Ye, J., and Qian, D. (2017). Telemedicine screening of retinal diseases with a handheld portable non-mydriatic fundus camera. *BMC Ophthalmology*, 17(1):89.

Kauppi, T. (2010). *Eye Fundus Image Analysis for Automatic Detection of Diabetic Retinopathy*.

Li, H., Esquivel, A., Davis, G., and Krupinski, E. (2006). Evaluation of digital resolution for viewing diabetic retinopathy microaneurysms.

Patton, N., Aslam, T., MacGillivray, T., Pattie, A., Deary, I. J., and Dhillon, B. (2005). Retinal vascular image analysis as a potential screening tool for cerebrovascular disease: a rationale based on homology between cerebral and retinal microvasculatures. *J Anat*, 206(4):319–348. 15817102[pmid].

Pérez, M. A., Bruce, B. B., Newman, N. J., and Biousse, V. (2012). The use of retinal photography in non-ophthalmic settings and its potential for neurology. *Neurologist*, 18(6):350–355. 23114666[pmid].

Phillips, C. I. (1984). Dilate the pupil and see the fundus. *Br Med J (Clin Res Ed)*, 288(6433):1779–1780. 6428541[pmid].

Quellec, G., Bazin, L., Cazuguel, G., Delafoy, I., Cochener, B., and Lamard, M. (2016). Suitability of a low-cost, handheld, nonmydriatic retinograph for diabetic retinopathy diagnosis. *Translational Vision Science & Technology*, 5(2):16.

Roorda, A. and Duncan, J. L. (2015). Adaptive optics ophthalmoscopy. *Annu Rev Vis Sci*, 1:19–50. 26973867[pmid].

Salz, D. A. and Witkin, A. J. (2015). Imaging in diabetic retinopathy. *Middle East African journal of ophthalmology*, 22(2):145.

Shen, B. Y. and Mukai, S. (2017). A portable, inexpensive, nonmydriatic fundus camera based on the raspberry pi® computer. *Journal of Ophthalmology*, 2017(3):5.

Swedish, T., Roesch, K., Lee, I., Rastogi, K., Bernstein, S., and Raskar, R. (2015). eyeselfie: Self directed eye alignment using reciprocal eye box imaging. *ACM Trans. Graph.*, 34(4).

Tarr, J. M., Kaul, K., Chopra, M., Kohner, E. M., and Chibber, R. (2013). Pathophysiology of Diabetic Retinopathy. *ISRN Ophthalmology*, 2013:1–13.

Tocci, M. (2007). How to model the human eye in zemax.

Tran, K., Mendel, T. A., Holbrook, K. L., and Yates, P. A. (2012). Construction of an inexpensive, hand-held fundus camera through modification of a consumer "point-and-shoot" camera. *Investigative ophthalmology & visual science*, 53 12:7600–7.

Volk Optical Inc. Volk InView.

Volk Optical Inc. Volk Pictor Plus.